



Hierarchical 0D–2D Co/Mo Selenides as Superior Bifunctional Electrocatalysts for Overall Water Splitting

Lu Xia^{1,2}, Hao Song¹, Xingxing Li¹, Xuming Zhang^{1*}, Biao Gao^{1,3}, Yang Zheng^{1*}, Kaifu Huo¹ and Paul K. Chu³

¹ The State Key Laboratory of Refractories and Metallurgy and Institute of Advanced Materials and Nanotechnology, Wuhan University of Science and Technology, Wuhan, China, ² The College of Resources and Environment Engineering, Wuhan University of Science and Technology, Wuhan, China, ³ Departments of Physics, Materials Science and Engineering, and Biomedical Engineering, City University of Hong Kong, Hong Kong, China

OPEN ACCESS

Edited by:

Guanglin Xia,
Fudan University, China

Reviewed by:

Shichun Mu,
Wuhan University of
Technology, China
Fei Ma,
Xi'an Jiaotong University, China

*Correspondence:

Xuming Zhang
xumzhang@wust.edu.cn
Yang Zheng
yzheng@wust.edu.cn

Specialty section:

This article was submitted to
Nanoscience,
a section of the journal
Frontiers in Chemistry

Received: 02 March 2020

Accepted: 14 April 2020

Published: 19 May 2020

Citation:

Xia L, Song H, Li X, Zhang X, Gao B,
Zheng Y, Huo K and Chu PK (2020)
Hierarchical 0D–2D Co/Mo Selenides
as Superior Bifunctional
Electrocatalysts for Overall Water
Splitting. *Front. Chem.* 8:382.
doi: 10.3389/fchem.2020.00382

Development of efficient electrocatalysts combining the features of low cost and high performance for both the hydrogen evolution reaction (HER) and oxygen evolution reaction (OER) still remains a critical challenge. Here, we proposed a facile strategy to construct *in situ* a novel hierarchical heterostructure composed of 0D–2D CoSe₂/MoSe₂ by the selenization of CoMoO₄ nanosheets grafted on a carbon cloth (CC). In such integrated structure, CoSe₂ nanoparticles dispersed well and tightly bonded with MoSe₂ nanosheets, which can not only enhance kinetics due to the synergetic effects, thus promoting the electrocatalytic activity, but also effectively improve the structural stability. Benefiting from its unique architecture, the designed CoSe₂/MoSe₂ catalyst exhibits superior OER and HER performance. Specifically, a small overpotential of 280 mV is acquired at a current density of 10 mA·cm⁻² for OER with a small Tafel slope of 86.8 mV·dec⁻¹, and the overpotential is 90 mV at a current density of 10 mA·cm⁻² for HER with a Tafel slope of 84.8 mV·dec⁻¹ in 1 M KOH. Furthermore, the symmetrical electrolyzer assembled with the CoSe₂/MoSe₂ catalysts depicts a small cell voltage of 1.63 V at 10 mA·cm⁻² toward overall water splitting.

Keywords: cobalt selenide, molybdenum selenide, hierarchical heterostructure, bifunctional electrocatalysts, overall water splitting

INTRODUCTION

Hydrogen is a promising energy source that boasts a high power density and environmental friendliness; therefore, electrolysis of water is hotly pursued as a renewable, efficient, and pollution-free technique (Amiinu et al., 2017; Luo et al., 2018; Zhu et al., 2018). Electrocatalytic water splitting consists of the hydrogen evolution reaction (HER) and oxygen evolution reaction (OER), and electrocatalysts as the chemical reaction centers play a critical role in the water splitting electrolyzer. Although some noble metal oxide catalysts (RuO₂ and IrO₂) have high electrocatalytic performance for the OER and some noble metal catalysts (Pt and Ir) deliver good electrochemical property in the HER, the high cost and scarcity restrict their wide industrial application (Trasatti, 1972, 1984). Therefore, noble-metal-free catalysts with high stability and efficiency are crucial to large-scale hydrogen production from water splitting. Currently, the OER activity in alkaline solution is the

bottleneck in overall water splitting due to the sluggish kinetics arising from the multiproton-coupled electron transfer steps (Jamesh and Sun, 2018). In practice, the HER catalyst in the electrolyzer should be compatible with the OER catalyst and functions in the same medium. Hence, development of suitable bifunctional noble-metal-free electrocatalysts with both high HER and OER performance in alkaline media is of great significance.

In recent years, transition metal dichalcogenides (TMDs) have attracted significant research interests owing to their earth-abundant reserves and acceptable activity for electrocatalytic HER (Xie et al., 2013; Zhang et al., 2017a; Xue et al., 2018; Wang et al., 2019). Particularly, layered MoSe₂ has been considered as a promising HER electrocatalyst because of its unique structure features and high electrochemical activity (Shi et al., 2015; Chen et al., 2018a; Zhang et al., 2018). Theoretical research has demonstrated that the Gibbs free energy for H atom absorption on the edge of MoSe₂ is lower than that of MoS₂ due to the more metallic nature of MoSe₂, revealing the higher HER performance (Tang et al., 2014; Lai et al., 2017; Yang et al., 2018). In addition, it also has been experimentally confirmed that the unsaturated Se edges in MoSe₂ nanosheets are extremely active as the S edges in MoS₂, which is responsible for the high HER activity (Jaramillo et al., 2007; Tang and Jiang, 2016). However, similar to MoS₂, the HER activity of layered MoSe₂ is largely limited by its poor conductivity and serious aggregation or restacking during the synthesis procedure (Mao et al., 2015; Qu et al., 2015), inhibiting the practical application of MoSe₂ catalyst. Therefore, it is significant to improve the electrochemical activity of MoSe₂-based catalyst. Recent works have shown that coupling MoSe₂ with other transition metal selenides and constructing heterostructured materials could be an effective approach to further enhance the electrochemical performance of MoSe₂. For instance, Wang et al. found that the MoSe₂@Ni_{0.85}Se nanowire delivered enhanced kinetics and performance for HER in alkaline conditions due to the high density of active edges of MoSe₂ and the good conductivity of Ni_{0.85}Se (Wang et al., 2017a). Zhang et al. synthesized 3D MoSe₂/NiSe₂ nanowires, which significantly enhanced HER activity with a low Tafel slope and overpotential in 0.5 M H₂SO₄, because the 3D structure affords more active sites (Zhang et al., 2017a). Liu et al. fabricated MoSe₂-NiSe₂@carbon heterostructures and achieved glorious HER catalytic properties and excellent durability in both acidic and base conditions (Liu et al., 2018). In addition, the hierarchical mesoporous MoSe₂@CoSe/N-C composite also exhibits outstanding HER activity (Chen et al., 2019b). Despite significant success, most of previous reports mainly focused on the improvement of HER performance, while the OER activity of MoSe₂ catalyst in alkaline media has been ignored. Hence, the rational design and fabrication of MoSe₂-based bifunctional electrocatalysts with satisfactory activity and stability toward overall water splitting in alkaline solution still remain a big challenge.

In this work, we developed a facile *in situ* phase separation strategy to construct a novel hierarchical heterostructure consisting of 0D–2D CoSe₂/MoSe₂ via the selenization of CoMoO₄ nanosheets supported on a carbon cloth (CC) (Figure 1). Due to the *in situ* phase transformation, CoSe₂

nanoparticles are uniformly anchored on MoSe₂ nanosheets in the integrated structure, which can not only enhance reaction kinetics because of the synergetic effects, thus boosting the electrocatalytic activity, but also effectively suppress the aggregation/restacking of MoSe₂ nanosheets, thereby improving the structural stability. Moreover, the hierarchical structure assembled by 0D–2D CoSe₂/MoSe₂ could provide abundant active sites for the electrochemical reactions. As a result, the designed CoSe₂/MoSe₂ architecture exhibits outstanding OER and HER performance in alkaline media. More specifically, a small overpotential of 280 mV is achieved at a current density of 10 mA·cm⁻² for OER with a small Tafel slope of 86.8 mV·dec⁻¹, and the overpotential is 90 mV at a current density of 10 mA·cm⁻² for HER with a Tafel slope of 84.8 mV·dec⁻¹ in 1 M KOH. Moreover, the symmetrical electrolyzer assembled with the CoSe₂/MoSe₂ catalysts delivers a small cell voltage of 1.63 V at 10 mA·cm⁻² toward overall water splitting.

EXPERIMENTAL SECTION

Synthesis of CoMoO₄ Nanosheet

Firstly, a pristine carbon cloth (CC) was treated with nitric acid solution overnight, subsequently ultrasonicated in deionized (DI) water and dried in an oven at 80°C for 2 h. After that, 1 mmol cobalt acetate, 1 mmol ammonium molybdate, 2 mmol urea, and 5 mmol ammonium fluoride were dissolved in 30 mL DI water, followed by ultrasonication for 30 min. Then, the homogeneous solution was poured into a 50-mL Teflon-lined stainless autoclave with the CC kept at 150°C for 6 h. After cooling to room temperature, the CC was washed with DI water for several times and dried in a vacuum freeze-dryer overnight. Finally, the obtained sample was treated at 400°C for 2 h with a ramp rate of 5°C min⁻¹ in an argon atmosphere.

Synthesis of CoSe₂/MoSe₂

The as-prepared CoMoO₄ precursor was reacted with 0.5 g selenium powder at 450°C for 1 h under an Ar/H₂ (90%/10%) atmosphere to form the CoSe₂/MoSe₂.

Synthesis of CoSe₂

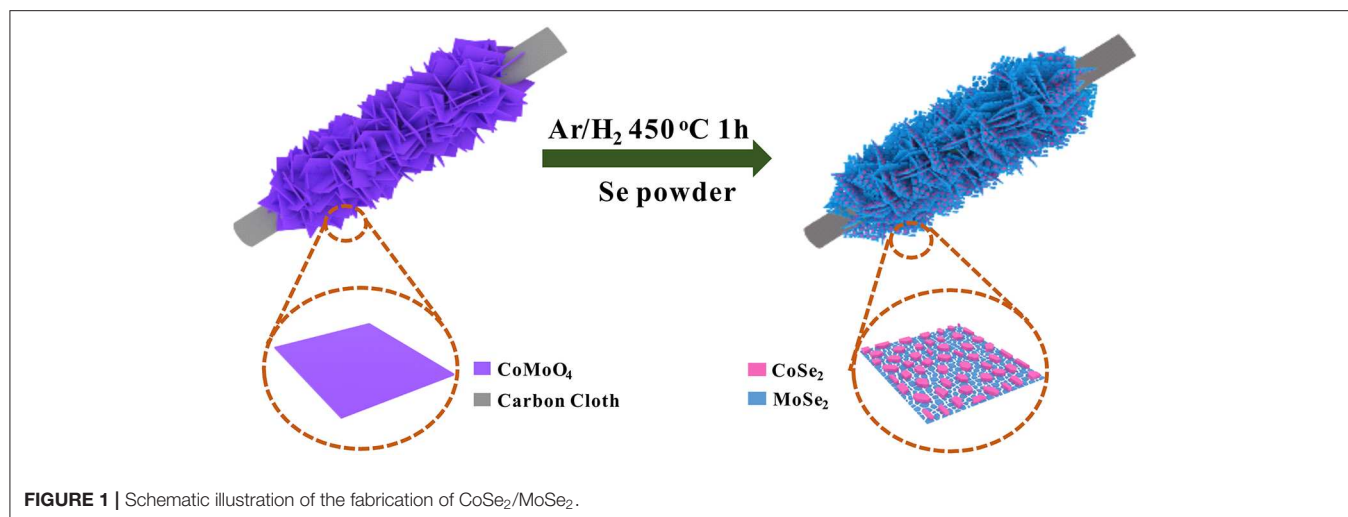
The CoSe₂ was prepared through two steps. Firstly, the treated CC was immersed in a 0.1 M Co(NO₃)₂ solution for the electrodeposition of Co (Yang et al., 2015). Then, the collected sample was reacted with 0.5 g selenium powder under an Ar/H₂ (90%/10%) atmosphere at 450°C for 1 h.

Synthesis of MoSe₂

Firstly, MoS₂ was prepared via hydrothermal reaction with the CC at 200°C for 12 h, followed by heating at 400°C for 2 h to form MoO₃ (Wu et al., 2018). Then, the obtained MoO₃ was reacted with 0.5 g selenium powder at 450°C for 1 h under an Ar/H₂ (90%/10%) atmosphere.

Preparation of Pt/C

Four milligrams of 20% Pt/C and 20 μL 5% Nafion solution were added into 1 mL solution of isopropanol and DI water (9:1) and then sonicated to form a uniform solution. Finally, the 1*1 cm²



CC was soaked in the homogeneous solution and dried in air at atmospheric temperature.

Preparation of RuO₂

Four milligrams of RuO₂ and 20 μ L 5% Nafion solution were added into 1 mL solution of isopropanol and DI water (9:1), and then the sample was sonicated to form a uniform solution. Finally, the 1*1 cm² CC was soaked in the homogeneous solution and dried in air at atmospheric temperature.

CHARACTERIZATION

The phase composition of the samples were characterized by X-ray diffraction (XRD, Bruker D8A A25), and the chemical states were determined through X-ray photoelectron spectroscopy (XPS, ESCALB 250Xi). The morphology and microstructure were recorded via field emission scanning electron microscopy (FE-SEM, FEI Nova NANOSEM 400) and high-resolution transmission electron microscopy (HR-TEM, JEM-2100 UHR STEM).

ELECTROCHEMICAL MEASUREMENTS

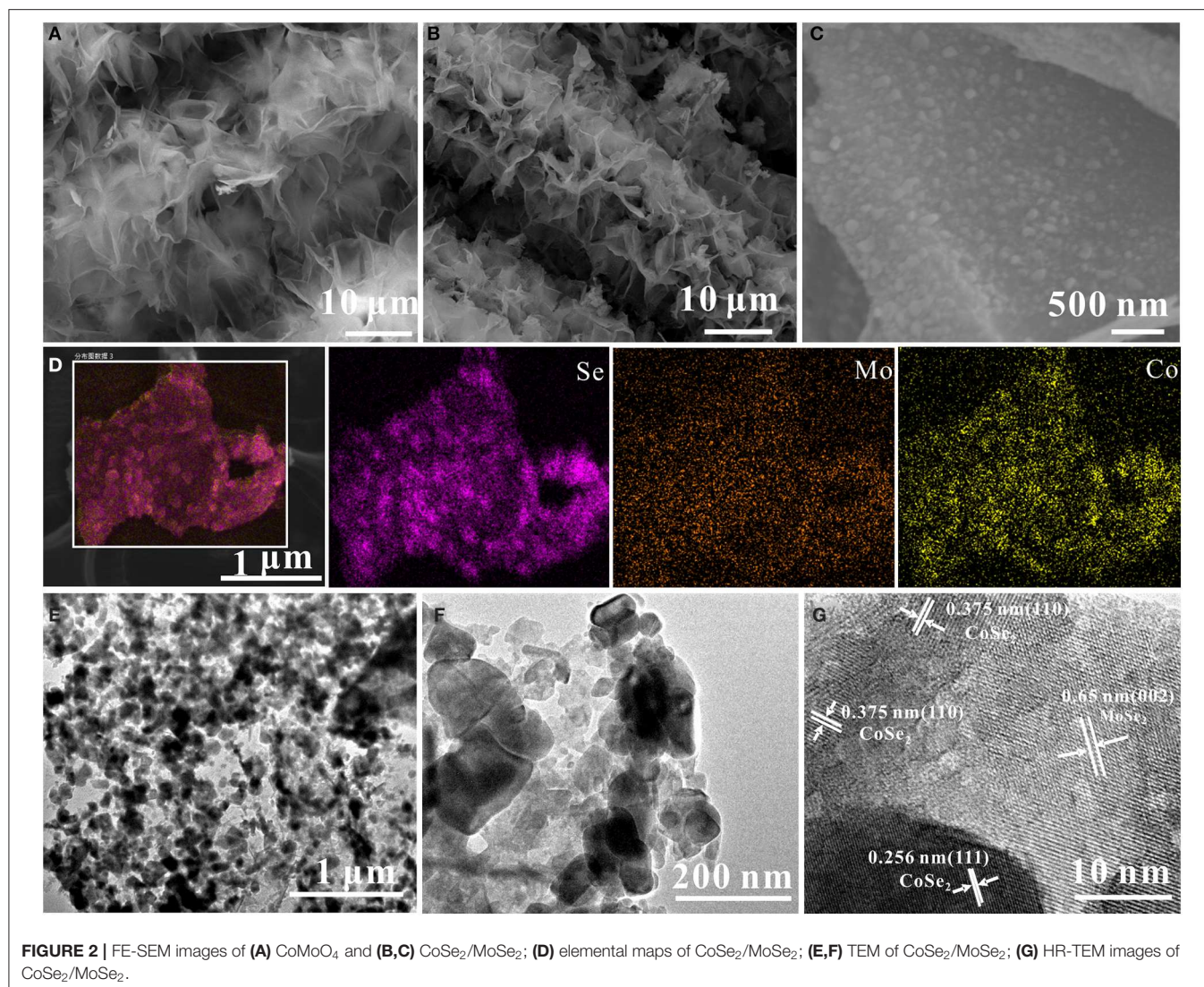
All samples made use of a three-electrode system performed by a biologic VSP300 type electrochemical workstation (Biologic Science Instruments, France). The sample of CoSe₂/MoSe₂ was put on the electrode holder as the working electrode with a mass loading of 4 mg/cm², the saturated calomel electrode (SCE) was the reference electrode, and a carbon rod served as the counter electrode. The electrolyte was 1 M KOH solution with saturated N₂. Linear sweep voltammetry (LSV) was characterized by polarization curves of OER with a scanning rate of 5 mV s⁻¹ from 0 to 0.8 V vs. SCE. Similarly, the polarization curves of HER were determined under the same condition from 0 to -0.8 V vs. SCE. The potentials were standardized by a reversible hydrogen electrode (RHE) as shown in the following: $E(\text{RHE}) = E(\text{SCE}) + 0.059 \times \text{pH}$ with instrument automatic 85% iR compensation. The electrochemically active

surface area (ECSA) was calculated by cyclic voltammetry (CV) performed from -0.3 to -0.2 V vs. SCE with different scanning rates of 40, 60, 80, 100, and 120 mV s⁻¹. Electrochemical impedance spectroscopy (EIS) measurements were conducted by biologic VMP3 (Biologic Science Instruments, France) from 100 KHz to 0.1 Hz. The overall water-splitting electrolyzer was performed with CoSe₂/MoSe₂ as electrodes and 1 M KOH as the electrolyte.

RESULTS AND DISCUSSION

Figure 2A presents the FE-SEM image of the as-prepared CoMoO₄ precursor, which presents uniform nanosheets (with a lateral size of 2 μ m) perpendicularly grown on the CC substrate with high coverage. After a selenization process, the obtained CoSe₂/MoSe₂ sample well maintains the pristine morphology of the CoMoO₄ precursor (**Figure 2B**). Moreover, the high-magnification SEM image further reveals that lots of nanoparticles are well dispersed on the surface of the nanosheet (**Figure 2C**), implying the structure and phase evolution during the selenization treatment. The elemental maps in (**Figure 2D**) show that Mo, Co, and Se are uniformly distributed throughout the nanosheets. In addition, the low-resolution TEM images in (**Figures 2E,F**) display that nanoparticles are uniformly distributed on the nanosheet during the thermal reduction procedure, forming the 0D/2D structure. Furthermore, the high-resolution TEM (**Figure 2G**) shows the lattice fringes of 0.26 nm and 0.65 nm corresponding to the (111) and (002) planes of CoSe₂ and MoSe₂, respectively (Qu et al., 2016; Liu et al., 2017), demonstrating the successful formation of the CoSe₂/MoSe₂ after the selenization reaction.

To investigate phase evolution during the selenization process, the crystal structure and phase composition of the obtained samples were characterized by X-ray diffraction (XRD) analysis (**Figure 3A**). The diffraction peaks of CoMoO₄ precursor (in the black line) can be well indexed to the CoMoO₄ phase (JCPDS No: 21-0868) (Wang et al., 2016). After the thermal reduction, some



new diffraction peaks can be observed. The diffraction peaks at around 13.7°, 27.6°, 31.4°, and 37.8° can be assigned to the MoSe₂ phase (JCPDS No: 77-1715) (Qu et al., 2016), while the other peaks could be attributed to the phase of CoSe₂ (JCPDS No:53-0449) (Liu et al., 2017). The XRD result clearly manifests the successful phase separation of the CoSe₂ and MoSe₂ from the CoMoO₄ precursor via the selenization process.

X-ray photoelectron spectroscopy (XPS) measurement was carried out to analyze the composition and chemical state of as-prepared samples. (Figure 3B) illustrates the high-resolution Co 2p peaks at 778.8 eV (Co 2p_{3/2}), 793.7 eV (Co 2p_{1/2}), 780 eV (Co 2p_{3/2}), and 796 eV (Co 2p_{1/2}), corresponding to CoSe₂ and cobalt–oxygen bond, while those peaks at 784.1 eV and 801.5 eV are the satellite peaks (Mu et al., 2016; Wang et al., 2017b; Gao et al., 2018). Furthermore, the fine Mo 3d XPS spectrum (Figure 3C) shows the main peaks at 228.8 eV and 231.9 eV, which represent the Mo 3d_{5/2} and Mo 3d_{3/2} of MoSe₂ (Wang et al., 2018a,b). Additionally, the peak located

at 230 eV can be ascribed to the Se 3s of MoSe₂ (Zhao et al., 2018). The Se 3d XPS spectrum (Figure 3D) displays the characteristic of CoSe₂ and MoSe₂ at 54.5 eV and 55.4 eV in agreement with the Se 3d_{5/2} and Se 3d_{3/2}, respectively (Gao et al., 2018). Moreover, the peak at around 59.8 eV is confirmed to correspond to the selenium–oxygen bond (Kong et al., 2014). According to these results, the selenization process induced the phase separation from CoMoO₄ into the nanoscale CoSe₂ and MoSe₂.

It is generally recognized that highly efficient electrocatalysts worked in alkaline solution is the bottleneck for large-scale application of overall water splitting. Linear sweep voltammetry (LSV) at a scanning rate of 5 mV s⁻¹ was characterized by the electrocatalytic HER and OER capacities of the samples by a three-electrode system in 1 M KOH solution with saturated N₂. By contrast, CoSe₂, MoSe₂ (Figure S1), RuO₂, and Pt/C catalysts were performed in the same condition. The HER polarization curves and corresponding Tafel slopes

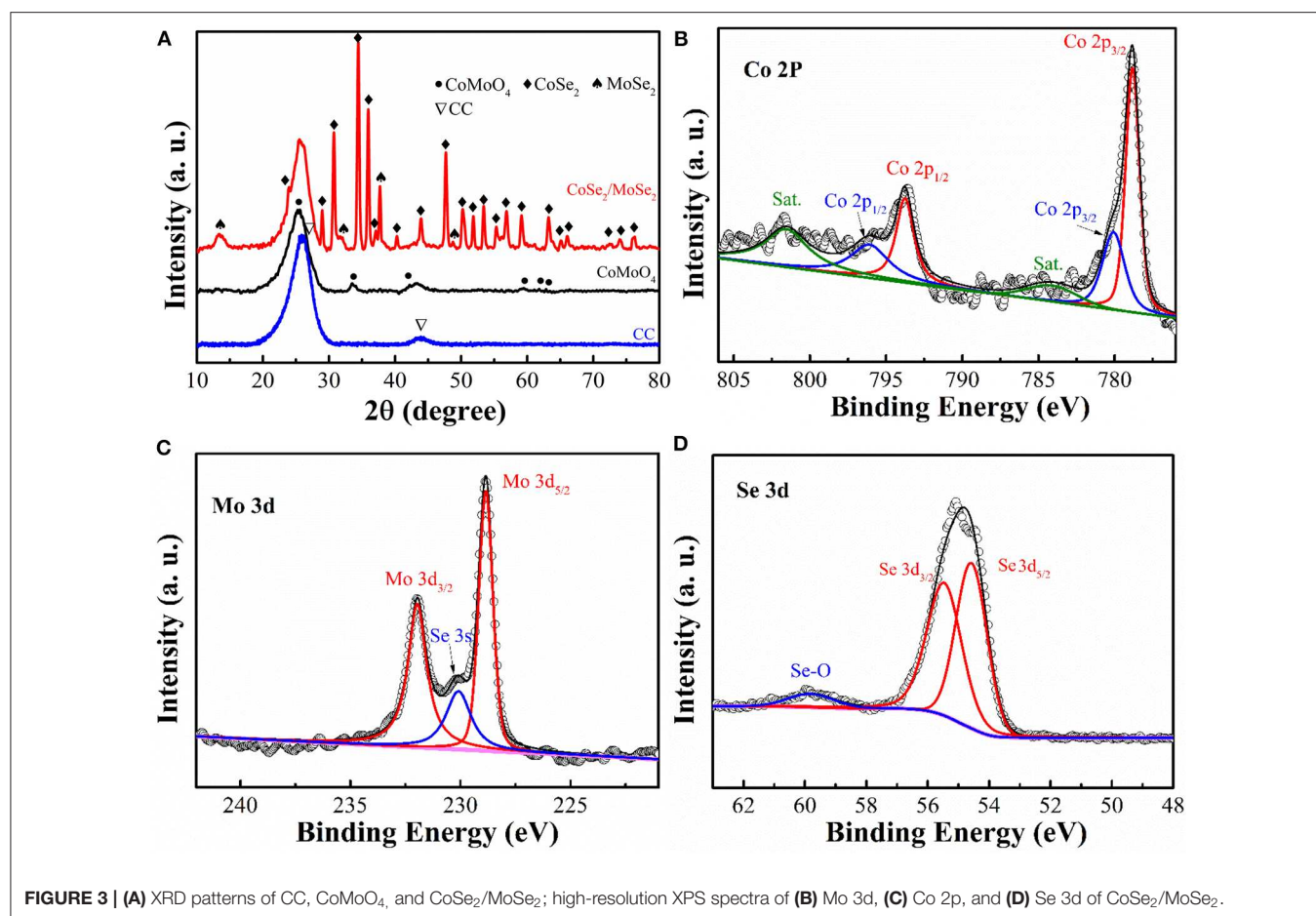
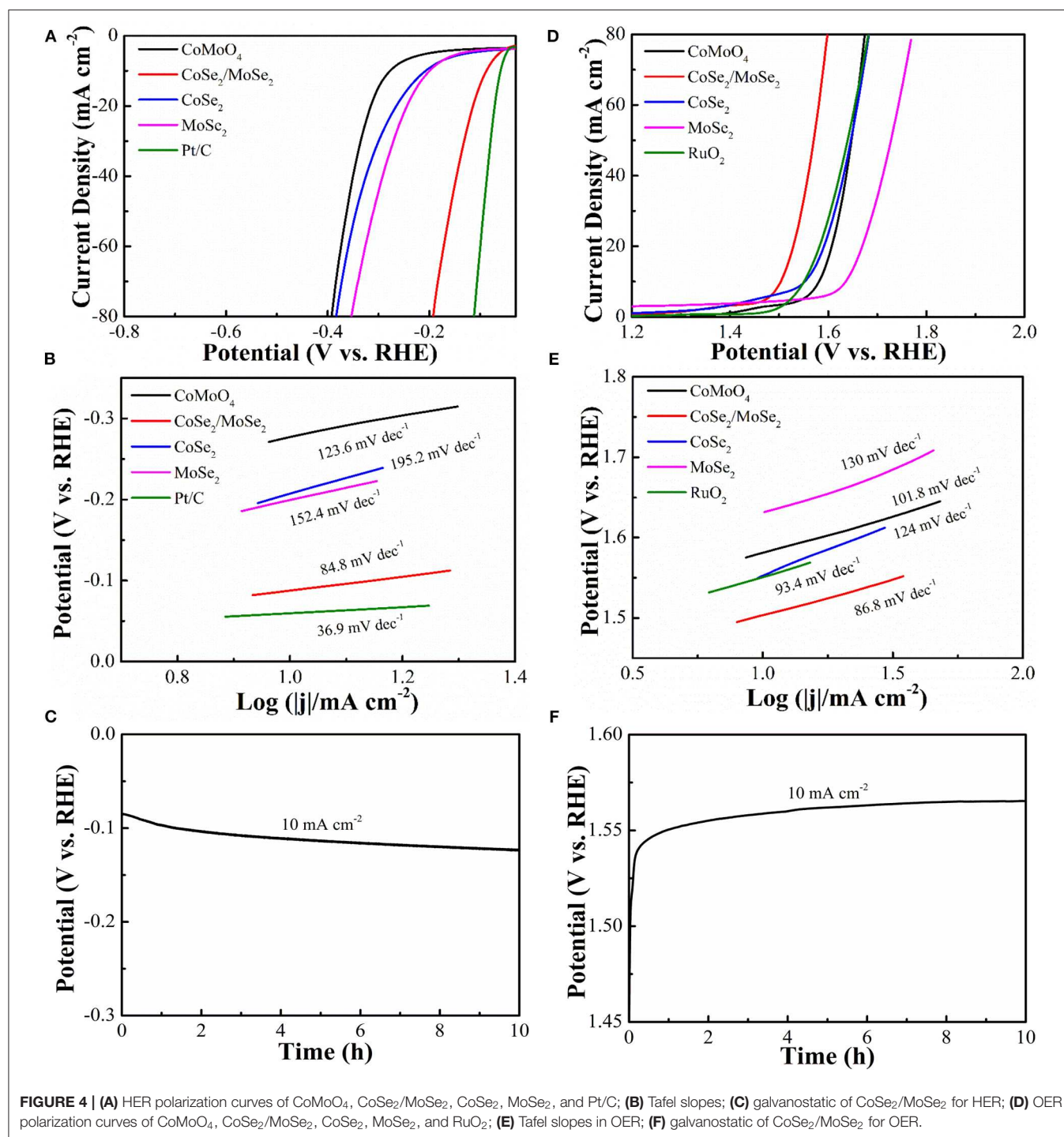


FIGURE 3 | (A) XRD patterns of CC, CoMoO₄, and CoSe₂/MoSe₂; high-resolution XPS spectra of (B) Mo 3d, (C) Co 2p, and (D) Se 3d of CoSe₂/MoSe₂.

are depicted in (Figures 4A,B). The overpotential (η_{10}) and Tafel slope of CoSe₂/MoSe₂ are 90 mV and 84.8 mV·dec⁻¹, which are better than those of CoMoO₄ (277 mV, 123.6 mV·dec⁻¹), CoSe₂ (205 mV, 195.2 mV·dec⁻¹), and MoSe₂ (199 mV, 152.4 mV·dec⁻¹). CoSe₂ has a metallic character, which can promote the dissociation of water and provide protons under alkaline conditions, thus improving the HER performance of MoSe₂ (Kwak et al., 2016). In addition, the hierarchical nanosheet array assembled by the CoSe₂/MoSe₂ provides abundant active sites for the electrochemical reaction at the phase interface, which can further enhance the HER performance (Zhang et al., 2017a). Therefore, the CoSe₂/MoSe₂ catalyst exhibits improved HER performance benefiting from the synergistic effect. The catalyst of Pt/C illustrates an overpotential (η_{10}) (59 mV) and Tafel slope (36.9 mV·dec⁻¹) in 1 M KOH that are similar to those in other literatures (Chen et al., 2018b; Wan et al., 2018). Moreover, the overpotential of CoSe₂/MoSe₂ is superior to those of recently reported selenide catalysts such as NiSe NWs/Ni Foam (96 mV) (Tang et al., 2015), EG/cobalt selenide/NiFe-LDH (260 mV) (Hou et al., 2016), o-CoSe₂/P (104 mV) (Zheng et al., 2018), CoSe₂ NCs (520 mV) (Kwak et al., 2016), Co_{0.75}Ni_{0.25}Se/NF (106 mV) (Liu et al., 2019), 1T MoSe₂/NiSe (120 mV) (Zhang

et al., 2019), and SWCNTs/MoSe₂ (219 mV) (Najafi et al., 2019) (Table S1).

The electrocatalytic OER properties are determined by LSV and polarization measurements as shown in (Figures 4D,E). The CoSe₂/MoSe₂ catalyst shows a lower overpotential (η_{10} of 280 mV) than those of the CoMoO₄ (352 mV), CoSe₂ (322 mV), MoSe₂ (404 mV), and RuO₂ (318 mV), respectively. More importantly, the OER performance of the designed CoSe₂/MoSe₂ sample exceeds those of recently reported selenide catalysts in OER, for instance, the Ag-CoSe₂ (320 mV) (Zhao et al., 2017), CoSe₂ NCs (430 mV) (Kwak et al., 2016), CoSe₂/DETA (392 mV) (Guo et al., 2017), NiCo₂Se₄ holey nanosheets (295 mV) (Fang et al., 2017), NiSe-Ni_{0.85}Se/CP (300 mV) (Chen et al., 2018a), SWCNTs/MoSe₂ (295 mV) (Najafi et al., 2019), 1T/2H MoSe₂ (397 mV) (Li et al., 2019), and CoSe₂@MoSe₂ (309 mV) (Chen et al., 2019c) (Table S2). Furthermore, the corresponding Tafel slope of CoSe₂/MoSe₂ is 86.8 mV·dec⁻¹, which is smaller than those of the CoMoO₄ (101.8 mV·dec⁻¹), CoSe₂ (124 mV·dec⁻¹), MoSe₂ (130 mV·dec⁻¹), and RuO₂ (93.4 mV·dec⁻¹). The CoSe₂/MoSe₂ has lower overpotential and smaller Tafel, which can be attributed to its unique hierarchical heterostructure, facilitating electron transfer and accelerating OER kinetics. In this heterostructure, the transfer of electrons from CoSe₂ phase to



MoSe₂ phase in the CoSe₂/MoSe₂ interface can result in electron-poor Co species and electron-rich Mo species (Liu et al., 2018). It is believed that the Se anion can affect the electron transfer between Co and Mo species, which is important for boosting catalytic ability (Yan et al., 2019). Besides, the formation of CoOOH is the primary cause to promote OER activity (Liu et al., 2015), and the increased 3d–4p repulsion between the center

of the metal d band and the center of the p band of the Se site further promotes the rapid transfer of dioxygen molecules, thus improving OER performance (Li et al., 2017).

To understand the effects of the structure and composition of prepared catalyst on the electrochemical performance, several CoSe₂/MoSe₂ catalysts were collected at different selenization temperatures and the HER and OER performance were evaluated

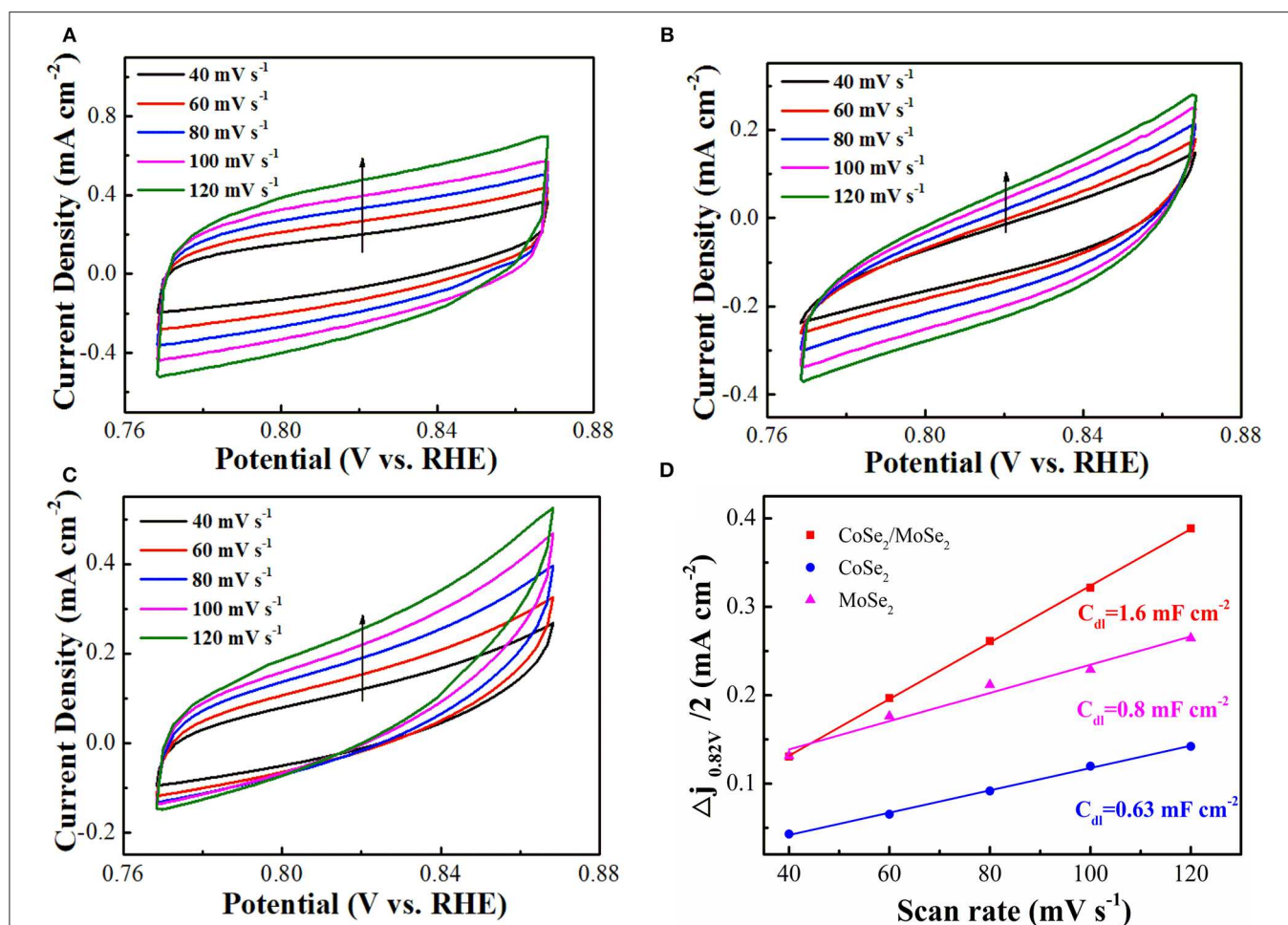


FIGURE 5 | Electrochemical double-layer capacitance with the CV curves acquired at different scanning rates from 40, 60, 80, 100, and 120 mV s^{-1} : **(A)** $\text{CoSe}_2/\text{MoSe}_2$, **(B)** CoSe_2 , and **(C)** MoSe_2 ; **(D)** current densities ($\Delta j = j_{\text{anode}} - j_{\text{cathode}}$, at 0.82 V) as a function of scanning rates of $\text{CoSe}_2/\text{MoSe}_2$, CoSe_2 , and MoSe_2 with the corresponding slope being twice that of the C_{dl} values.

by LSV analysis (Figure S2). It can be seen that the $\text{CoSe}_2/\text{MoSe}_2$ sample obtained at 450°C ($\text{CoSe}_2/\text{MoSe}_2\text{-}450$) possesses better electrocatalytic properties than other counterparts, which can be ascribed to its superior structure. As shown in (Figure S3), with the selenization temperature increasing, the size of nanoparticles on the surface of nanosheets increased as well, indicating higher crystallinity. Generally, larger particle size will reduce the active surface of catalyst (Zhang et al., 2017b; Chen et al., 2019a). Therefore, when the selenization temperature elevated to 500°C ($\text{CoSe}_2/\text{MoSe}_2\text{-}500$), the catalytic performance slightly declined owing to its larger particle size and lower active surface. In addition, (Figure S4) displays the composition of the $\text{CoSe}_2/\text{MoSe}_2$ catalysts achieved at a different selenization temperature. As can be seen, when the selenization process proceeded at low temperature, the obtained $\text{CoSe}_2/\text{MoSe}_2$ catalyst has poor MoSe_2 phase and low crystallinity, which are responsible for the poor electrochemical catalytic performance of the catalysts ($\text{CoSe}_2/\text{MoSe}_2\text{-}350$ and $\text{CoSe}_2/\text{MoSe}_2\text{-}400$). Therefore, the catalyst synthesized at 450°C shows the best

performance, benefiting from the appropriate crystal structure and phase composition.

The electrochemically active surface area (ECSA) of as-prepared catalyst was evaluated by the double-layer capacitance (C_{dl}), which was measured by CV in a non-Faradaic reaction potential range (Deng et al., 2015). The C_{dl} values of the $\text{CoSe}_2/\text{MoSe}_2$ (1.6 mF cm^{-2}) is higher than those of CoSe_2 (0.63 mF cm^{-2}) and MoSe_2 (0.8 mF cm^{-2}), as shown in (Figure 5), suggesting more active sites of the $\text{CoSe}_2/\text{MoSe}_2$ catalyst. Furthermore, the smaller R_{ct} value for the $\text{CoSe}_2/\text{MoSe}_2$ catalyst in the EIS measurement (Figure S5) implies the promoted charge transfer and boosted kinetics, which can be ascribed to the abundant interfaces and synergetic effect between the CoSe_2 and MoSe_2 .

The structural stability is another significant parameter for catalysts in HER and OER. (Figures 4C,F) show a galvanostatic for $\text{CoSe}_2/\text{MoSe}_2$ catalyst in both the HER and OER processes. The morphology and composition of the catalyst after galvanostatic cycling are characterized by SEM and XPS. The

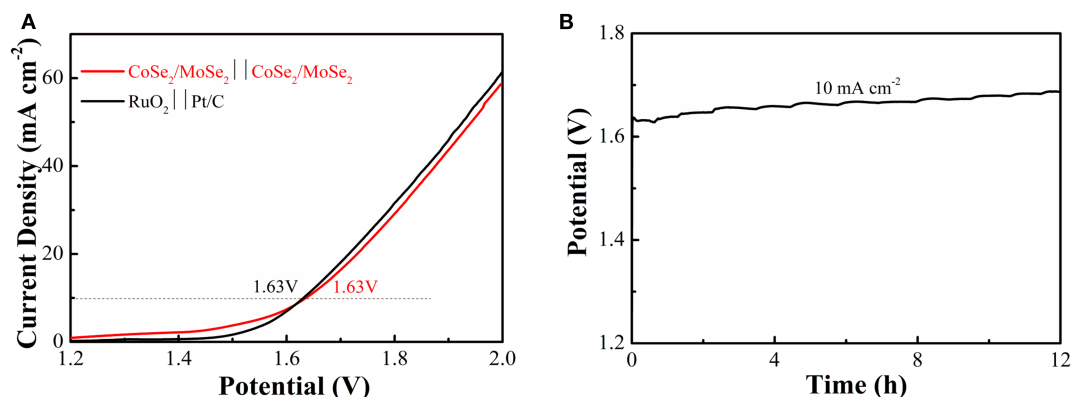


FIGURE 6 | (A) LSV curves of water splitting with CoSe₂/MoSe₂ as the anode and cathode; **(B)** galvanostatic testing of the CoSe₂/MoSe₂-based water splitting electrolyzer for 12 h at 10 mA cm⁻².

CoSe₂/MoSe₂ could well inherit the pristine sheet-like structure, demonstrating good structural stability. In addition, the fine XPS spectra of the Co 2p, Mo 3d, Se 3d acquired from the sample of CoSe₂/MoSe₂ after galvanostatic measurement confirm the reservation of CoSe₂ and MoSe₂ (Figure S6), indicating phase stability during the electrochemical reactions.

To investigate its practical application of the obtained catalyst, an overall water splitting electrolyzer is assembled with CoSe₂/MoSe₂ as electrodes in 1 M KOH. It can decompose water at a low cell voltage of 1.63 V (current density at 10 mA·cm⁻²) (Figure 6A), and the efficiency is similar to those constituting of the noble-metal-based cathode and anode (RuO₂ vs. Pt/C). Moreover, the overall water splitting performance of the CoSe₂/MoSe₂ is better than those of other recently reported non-noble metals at the same current density, such as (Ni,Co)_{0.85}Se NSAs (1.65 V) (Xiao et al., 2018), a-CoSe/Ti mesh (1.65 V) (Liu et al., 2015), CoO_x-CoSe (1.64 V) (Xu et al., 2016), Co_{0.85}Se@NC (1.76 V) (Meng et al., 2017), CoB₂/CoSe₂ (1.73 V) (Guo et al., 2017), NiSe₂/Ni (1.64 V) (Zhang et al., 2018), 1T/2H MoSe₂/MXene (1.64 V) (Li et al., 2019), and Ni₃Se₂/CF (1.65 V) (Shi et al., 2015) (Table S3). Additionally, CoSe₂/MoSe₂ electrolyzer exhibits a slight increase in the potential after being cycled for 12 h in alkaline solution (Figure 6B).

CONCLUSION

In summary, a novel hierarchical 0D–2D Co/Mo selenide was developed by a facile *in situ* phase separation strategy. Benefiting from its unique structure and composition, the constructed CoSe₂/MoSe₂ catalyst exhibits small η_{10} of 280 mV and 90 mV

and Tafel slopes of 86.8 mV·dec⁻¹ and 84.8 mV·dec⁻¹ for OER and HER, respectively. Furthermore, the electrolyzer comprising CoSe₂/MoSe₂ as the bifunctional catalyst shows a small water splitting cell voltage of 1.63 V at a current density of 10 mA·cm⁻². This work provides insights into rational design and development of economical and valid bifunctional catalysts for overall water splitting.

DATA AVAILABILITY STATEMENT

All datasets generated for this study are included in the article/Supplementary Material.

AUTHOR CONTRIBUTIONS

LX implemented the experiment, analyzed the data and wrote the article. HS, XL, XZ, and BG participated in the formulation of the experimental scheme. YZ, KH, and PC revised the article.

FUNDING

This work was financially supported by the National Natural Science Foundation of China (Nos. 51572100, 61434001, and 31500783).

SUPPLEMENTARY MATERIAL

The Supplementary Material for this article can be found online at: <https://www.frontiersin.org/articles/10.3389/fchem.2020.00382/full#supplementary-material>

REFERENCES

- Amiin, I. S., Pu, Z., Liu, X., Owusu, K. A., Monestel, H. G. R., Boakye, F. O., et al. (2017). Multifunctional Mo–N/C@MoS₂ electrocatalysts for her, oer, orr, and Zn–air batteries. *Adv. Funct. Mater.* 27:1702300. doi: 10.1002/adfm.201702300
- Chen, J., Ge, Y., Feng, Q., Zhuang, P., Chu, H., Cao, Y., et al. (2019a). Nesting Co₃Mo binary alloy nanoparticles onto molybdenum oxide nanosheet arrays for superior hydrogen evolution reaction. *ACS Appl. Mater. Interfaces* 11, 9002–9010. doi: 10.1021/acsami.8b19148
- Chen, J., Pan, A., Wang, Y., Cao, X., Zhang, W., Kong, X., et al. (2019b). Hierarchical mesoporous MoSe₂@CoSe/N-doped carbon nanocomposite for

- sodium ion batteries and hydrogen evolution reaction applications. *Energy Storage Mater.* 21, 97–106. doi: 10.1016/j.ensm.2018.10.019
- Chen, Y., Ren, Z., Fu, H., Zhang, X., Tian, G., and Fu, H. (2018a). NiSe-Ni_{0.85}Se heterostructure nanoflake arrays on carbon paper as efficient electrocatalysts for overall water splitting. *Small* 14:1800763. doi: 10.1002/smll.201800763
- Chen, Z., Wang, W., Huang, S., Ning, P., Wu, Y., Gao, C., et al. (2019c). Well-defined CoSe₂@MoSe₂ hollow heterostructured nanocubes with enhanced dissociation kinetics for overall water splitting. *Nanoscale* 12, 326–335. doi: 10.1039/C9NR08751F
- Chen, Z., Wu, R., Liu, Y., Ha, Y., Guo, Y., Sun, D., et al. (2018b). Ultrafine Co nanoparticles encapsulated in carbon-nanotubes-grafted graphene sheets as advanced electrocatalysts for the hydrogen evolution reaction. *Adv. Mater.* 30:1802011. doi: 10.1002/adma.201802011
- Deng, Z. H., Li, L., Ding, W., Xiong, K., and Wei, Z. D. (2015). Synthesized ultrathin MoS₂ nanosheets perpendicular to graphene for catalysis of hydrogen evolution reaction. *Chem. Commun.* 51, 1893–1896. doi: 10.1039/C4CC08491H
- Fang, Z., Peng, L., Lv, H., Zhu, Y., Yan, C., Wang, S., et al. (2017). Metallic transition metal selenide holey nanosheets for efficient oxygen evolution electrocatalysis. *ACS Nano* 11, 9550–9557. doi: 10.1021/acsnano.7b05481
- Gao, J., Li, Y., Shi, L., Li, J., and Zhang, G. (2018). Rational design of hierarchical nanotubes through encapsulating CoSe₂ nanoparticles into MoSe₂/C composite shells with enhanced lithium and sodium storage performance. *ACS Appl. Mater. Interfaces* 10, 20635–20642. doi: 10.1021/acami.8b06442
- Guo, Y., Yao, Z., Shang, C., and Wang, E. (2017). Amorphous Co₂B grown on CoSe₂ nanosheets as a hybrid catalyst for efficient overall water splitting in alkaline medium. *ACS Appl. Mater. Interfaces* 9, 39312–39317. doi: 10.1021/acami.7b10605
- Hou, Y., Lohe, M. R., Zhang, J., Liu, S., Zhuang, X., and Feng, X. (2016). Vertically oriented cobalt selenide/NiFe layered-double-hydroxide nanosheets supported on exfoliated graphene foil: an efficient 3D electrode for overall water splitting. *Energy Environ. Sci.* 9, 478–483. doi: 10.1039/C5EE03440J
- James, M. I., and Sun, X. (2018). Recent progress on earth abundant electrocatalysts for oxygen evolution reaction (OER) in alkaline medium to achieve efficient water splitting—a review. *J. Power Sources* 400, 31–68. doi: 10.1016/j.jpowsour.2018.07.125
- Jaramillo, T. F., Jørgensen, K. P., Bonde, J., Nielsen, J. H., Horch, S., and Chorkendorff, I. (2007). Identification of active edge sites for electrochemical H₂ evolution from MoS₂ nanocatalysts. *Science* 317:100. doi: 10.1126/science.1141483
- Kong, D., Wang, H., Lu, Z., and Cui, Y. (2014). CoSe₂ nanoparticles grown on carbon fiber paper: an efficient and stable electrocatalyst for hydrogen evolution reaction. *J. Am. Chem. Soc.* 136, 4897–4900. doi: 10.1021/ja501497n
- Kwak, I. H., Im, H. S., Jang, D. M., Kim, Y. W., Park, K., Lim, Y. R., et al. (2016). CoSe₂ and NiSe₂ nanocrystals as superior bifunctional catalysts for electrochemical and photoelectrochemical water splitting. *ACS Appl. Mater. Interfaces* 8, 5327–5334. doi: 10.1021/acami.5b12093
- Lai, F., Yong, D., Ning, X., Pan, B., Miao, Y. E., and Liu, T. (2017). Bionanofiber assisted decoration of few-layered MoSe₂ nanosheets on 3D conductive networks for efficient hydrogen evolution. *Small* 13:1602866. doi: 10.1002/smll.201602866
- Li, N., Zhang, Y., Jia, M., Lv, X., Li, X., Li, R., et al. (2019). 1T/2H MoSe₂-on-MXene heterostructure as bifunctional electrocatalyst for efficient overall water splitting. *Electrochim. Acta* 326:134976. doi: 10.1016/j.electacta.2019.134976
- Li, W., Gao, X., Xiong, D., Wei, F., Song, W. G., Xu, J., et al. (2017). Hydrothermal synthesis of monolithic Co₃Se₄ nanowire electrodes for oxygen evolution and overall water splitting with high efficiency and extraordinary catalytic stability. *Adv. Energy Mater.* 7:1602579. doi: 10.1002/aenm.201602579
- Liu, C., Wang, K., Zheng, X., Liu, X., Liang, Q., and Chen, Z. (2018). Rational design of MoSe₂-NiSe₂@carbon heterostructures for efficient electrocatalytic hydrogen evolution in both acidic and alkaline media. *Carbon* 139, 1–9. doi: 10.1016/j.carbon.2018.06.034
- Liu, S., Jiang, Y., Yang, M., Zhang, M., Guo, Q., Shen, W., et al. (2019). Highly conductive and metallic cobalt-nickel selenide nanorods supported on Ni foam as an efficient electrocatalyst for alkaline water splitting. *Nanoscale* 11, 7959–7966. doi: 10.1039/C8NR10545F
- Liu, T., Liu, Q., Asiri, A. M., Luo, Y., and Sun, X. (2015). An amorphous CoSe film behaves as an active and stable full water-splitting electrocatalyst under strongly alkaline conditions. *Chem. Commun.* 51, 16683–16686. doi: 10.1039/C5CC06892
- Liu, X., Liu, Y., and Fan, L. Z. (2017). MOF-derived CoSe₂ microspheres with hollow interiors as high-performance electrocatalysts for the enhanced oxygen evolution reaction. *J. Mater. Chem. A* 5, 15310–15314. doi: 10.1039/C7TA04662F
- Luo, Y., Li, X., Cai, X., Zou, X., Kang, F., Cheng, H. M., et al. (2018). Two-dimensional MoS₂ confined Co(OH)₂ electrocatalysts for hydrogen evolution in alkaline electrolytes. *ACS Nano* 12, 4565–4573. doi: 10.1021/acsnano.8b00942
- Mao, S., Wen, Z., Ci, S., Guo, X., Ostrikov, K., and Chen, J. (2015). Perpendicularly oriented MoSe₂/graphene nanosheets as advanced electrocatalysts for hydrogen evolution. *Small* 11, 414–419. doi: 10.1002/smll.201401598
- Meng, T., Qin, J., Wang, S., Zhao, D., Mao, B., and Cao, M. (2017). In situ coupling of Co_{0.85}Se and N-doped carbon via one-step selenization of metal-organic frameworks as a trifunctional catalyst for overall water splitting and Zn-air batteries. *J. Mater. Chem. A* 5, 7001–7014. doi: 10.1039/C7TA01453H
- Mu, C. H., Qi, H. X., Song, Y. Q., Liu, Z. P., Ji, L. X., Deng, J. G., et al. (2016). One-pot synthesis of nanosheet-assembled hierarchical MoSe₂/CoSe₂ microcages for the enhanced performance of electrocatalytic hydrogen evolution. *RSC Adv.* 6, 23–30. doi: 10.1039/C5RA21638A
- Najafi, L., Bellani, S., Oropesa-Núñez, R., Prato, M., Martín-García, B., Brescia, R., et al. (2019). Carbon nanotube-supported MoSe₂ holey flake: Mo₂C ball hybrids for bifunctional pH-universal water splitting. *ACS Nano* 13, 3162–3176. doi: 10.1021/acsnano.8b08670
- Qu, B., Li, C., Zhu, C., Wang, S., Zhang, X., and Chen, Y. (2016). Growth of MoSe₂ nanosheets with small size and expanded spaces of (002) plane on the surfaces of porous N-doped carbon nanotubes for hydrogen production. *Nanoscale* 8, 16886–16893. doi: 10.1039/C6NR04619C
- Qu, B., Yu, X., Chen, Y., Zhu, C., Li, C., Yin, Z., et al. (2015). Ultrathin MoSe₂ nanosheets decorated on carbon fiber cloth as binder-free and high-performance electrocatalyst for hydrogen evolution. *ACS Appl. Mater. Interfaces* 7, 14170–14175. doi: 10.1021/acami.5b02753
- Shi, J., Hu, J., Luo, Y., Sun, X., and Asiri, A. M. (2015). Ni₃Se₂ film as a non-precious metal bifunctional electrocatalyst for efficient water splitting. *Catal. Sci. Technol.* 5, 4954–4958. doi: 10.1039/C5CY01121C
- Tang, C., Cheng, N., Pu, Z., Xing, W., and Sun, X. (2015). NiSe nanowire film supported on nickel foam: an efficient and stable 3D bifunctional electrode for full water splitting. *Angew. Chem. Int. Ed.* 54, 9351–9355. doi: 10.1002/anie.201503407
- Tang, H., Dou, K., Kaun, C. C., Kuang, Q., and Yang, S. (2014). MoSe₂ nanosheets and their graphene hybrids: synthesis, characterization and hydrogen evolution reaction studies. *J. Mater. Chem. A* 2, 360–364. doi: 10.1039/C3TA13584E
- Tang, Q., and Jiang, D. E. (2016). Mechanism of hydrogen evolution reaction on 1T-MoS₂ from first principles. *ACS Catal.* 6, 4953–4961. doi: 10.1021/acscatal.6b01211
- Trasatti, S. (1972). Work function, electronegativity, and electrochemical behaviour of metals: iii. electrolytic hydrogen evolution in acid solutions. *J. Electroanal. Chem.* 39, 163–184. doi: 10.1016/S0022-0728(72)80485-6
- Trasatti, S. (1984). Electrocatalysis in the anodic evolution of oxygen and chlorine. *Electrochim. Acta* 29, 1503–1512. doi: 10.1016/0013-4686(84)85004-5
- Wan, S., Jin, W., Guo, X., Mao, J., Zheng, L., Zhao, J., et al. (2018). Self-templating construction of porous CoSe₂ nanosheet arrays as efficient bifunctional electrocatalysts for overall water splitting. *ACS Sustain. Chem. Eng.* 6, 15374–15382. doi: 10.1021/acssuschemeng.8b03804
- Wang, B., Li, S., Wu, X., Liu, J., Tian, W., and Chen, J. (2016). Self-assembly of ultrathin mesoporous CoMoO₄ nanosheet networks on flexible carbon fabric as a binder-free anode for lithium-ion batteries. *New J. Chem.* 40, 2259–2267. doi: 10.1039/c5nj02910d
- Wang, B., Wang, Z., Wang, X., Zheng, B., Zhang, W., and Chen, Y. (2018a). Scalable synthesis of porous hollow CoSe₂-MoSe₂/carbon microspheres for highly efficient hydrogen evolution reaction in acidic and alkaline media. *J. Mater. Chem. A* 6, 12701–12707. doi: 10.1039/C8TA03523G
- Wang, C., Zhang, P., Lei, J., Dong, W., and Wang, J. (2017a). Integrated 3D MoSe₂@Ni_{0.85}Se nanowire network with synergistic cooperation as highly efficient electrocatalysts for hydrogen evolution reaction in alkaline medium. *Electrochim. Acta* 246, 712–719. doi: 10.1016/j.electacta.2017.06.028

- Wang, P., Pu, Z., Li, W., Zhu, J., Zhang, C., Zhao, Y., et al. (2019). Coupling NiSe₂-Ni₂P heterostructure nanowrinkles for highly efficient overall water splitting. *J. Catal.* 377, 600–608. doi: 10.1016/j.jcat.2019.08.005
- Wang, X., Li, F., Li, W., Gao, W., Tang, Y., and Li, R. (2017b). Hollow bimetallic cobalt-based selenide polyhedrons derived from metal-organic framework: an efficient bifunctional electrocatalyst for overall water splitting. *J. Mater. Chem. A* 5, 17982–17989. doi: 10.1039/C7TA03167J
- Wang, X., Zheng, B., Yu, B., Wang, B., Hou, W., Zhang, W., et al. (2018b). In situ synthesis of hierarchical MoSe₂-CoSe₂ nanotubes as an efficient electrocatalyst for the hydrogen evolution reaction in both acidic and alkaline media. *J. Mater. Chem. A* 6, 7842–7850. doi: 10.1039/C8TA01552J
- Wu, K., Zhan, J., Xu, G., Zhang, C., Pan, D., and Wu, M. (2018). MoO₃ nanosheet arrays as superior anode materials for Li- and Na-ion batteries. *Nanoscale* 10, 16040–16049. doi: 10.1039/C8NR03372B
- Xiao, K., Zhou, L., Shao, M., and Wei, M. (2018). Fabrication of (Ni,Co)_{0.85}Se nanosheet arrays derived from layered double hydroxides toward largely enhanced overall water splitting. *J. Mater. Chem. A* 6, 7585–7591. doi: 10.1039/C8TA01067F
- Xie, J., Zhang, H., Li, S., Wang, R., Sun, X., Zhou, M., et al. (2013). Defect-rich MoS₂ ultrathin nanosheets with additional active edge sites for enhanced electrocatalytic hydrogen evolution. *Adv. Mater.* 25, 5807–5813. doi: 10.1002/adma.201302685
- Xu, X., Du, P., Chen, Z., and Huang, M. (2016). An electrodeposited cobalt-selenide-based film as an efficient bifunctional electrocatalyst for full water splitting. *J. Mater. Chem. A* 4, 10933–10939. doi: 10.1039/C6TA03788G
- Xue, X., Zhang, J., Saana, I. A., Sun, J., Xu, Q., and Mu, S. (2018). Rational inert-basal-plane activating design of ultrathin 1T' phase MoS₂ with a MoO₃ heterostructure for enhancing hydrogen evolution performances. *Nanoscale* 10, 16531–16538. doi: 10.1039/C8NR05270K
- Yan, H., Xie, Y., Wu, A., Cai, Z., Wang, L., Tian, C., et al. (2019). Anion-modulated HER and OER activities of 3D Ni-V-based interstitial compound heterojunctions for high-efficiency and stable overall water splitting. *Adv. Mater.* 31:1901174. doi: 10.1002/adma.201901174
- Yang, L. J., Deng, Y. Q., Zhang, X. F., Liu, H., and Zhou, W. J. (2018). MoSe₂ nanosheet/MoO₂ nanobelt/carbon nanotube membrane as flexible and multifunctional electrodes for full water splitting in acidic electrolyte. *Nanoscale* 10, 9268–9275. doi: 10.1039/C8NR01572D
- Yang, X., Lu, A. Y., Zhu, Y., Hedhili, M. N., Min, S., Huang, K. W., et al. (2015). CoP nanosheet assembly grown on carbon cloth: a highly efficient electrocatalyst for hydrogen generation. *Nano Energy* 15, 634–641. doi: 10.1016/j.nanoen.2015.05.026
- Zhang, J., Wang, Y., Zhang, C., Gao, H., Lv, L., Han, L., et al. (2018). Self-supported porous NiSe₂ nanowrinkles as efficient bifunctional electrocatalysts for overall water splitting. *ACS Sustainable Chem. Eng.* 6, 2231–2239. doi: 10.1021/acssuschemeng.7b03657
- Zhang, L., Wang, T., Sun, L., Sun, Y., Hu, T., Xu, K., et al. (2017a). Hydrothermal synthesis of 3D hierarchical MoSe₂/NiSe₂ composite nanowires on carbon fiber paper and their enhanced electrocatalytic activity for the hydrogen evolution reaction. *J. Mater. Chem. A* 5, 19752–19759. doi: 10.1039/C7TA05352E
- Zhang, Q., Li, P., Zhou, D., Chang, Z., Kuang, Y., and Sun, X. (2017b). Superaerophobic ultrathin Ni-Mo alloy nanosheet array from in situ topotactic reduction for hydrogen evolution reaction. *Small* 13:1701648. doi: 10.1002/smll.201701648
- Zhang, X., Zhang, Y. Y., Zhang, Y., Jiang, W. J., Zhang, Q. H., Yang, Y. G., et al. (2019). Phase-controlled synthesis of 1T-MoSe₂/NiSe heterostructure nanowire arrays via electronic injection for synergistically enhanced hydrogen evolution. *Small Methods* 3:1800317. doi: 10.1002/smt.201800317
- Zhao, G., Li, P., Rui, K., Chen, Y., Dou, S. X., and Sun, W. (2018). CoSe₂/MoSe₂ heterostructures with enriched water adsorption/dissociation sites towards enhanced alkaline hydrogen evolution reaction. *Chem. Eur. J.* 24, 11158–11165. doi: 10.1002/chem.201801693
- Zhao, X., Zhang, H., Yan, Y., Cao, J., Li, X., Zhou, S., et al. (2017). Engineering the electrical conductivity of lamellar silver-doped cobalt(II) selenide nanobelts for enhanced oxygen evolution. *Angew. Chem. Int. Ed.* 56, 328–332. doi: 10.1002/anie.201609080
- Zheng, Y. R., Wu, P., Gao, M. R., Zhang, X. L., Gao, F. Y., Ju, H. X., et al. (2018). Doping-induced structural phase transition in cobalt diselenide enables enhanced hydrogen evolution catalysis. *Nat. Commun.* 9:2533. doi: 10.1038/s41467-018-04954-7
- Zhu, C., Wang, A. L., Xiao, W., Chao, D., Zhang, X., Tjep, N. H., et al. (2018). In situ grown epitaxial heterojunction exhibits high-performance electrocatalytic water splitting. *Adv. Mater.* 30:1705516. doi: 10.1002/adma.201705516

Conflict of Interest: The authors declare that the research was conducted in the absence of any commercial or financial relationships that could be construed as a potential conflict of interest.

Copyright © 2020 Xia, Song, Li, Zhang, Gao, Zheng, Huo and Chu. This is an open-access article distributed under the terms of the Creative Commons Attribution License (CC BY). The use, distribution or reproduction in other forums is permitted, provided the original author(s) and the copyright owner(s) are credited and that the original publication in this journal is cited, in accordance with accepted academic practice. No use, distribution or reproduction is permitted which does not comply with these terms.